FEM-FCT Based Dynamic Simulation of Corona Discharge in Point-Plane Configuration

P. Sattari, G.S.P. Castle, *Life Fellow, IEEE*, and K. Adamiak, *Fellow, IEEE*

***Abstract*—In this paper, a numerical algorithm for the simulation of the dynamic corona discharge in air is proposed assuming single species charge carriers. The simulation results show the behavior of corona current and space charge density under two waveforms of the applied voltage: step and pulse. The electric field is calculated by means of the Finite Element Method and the Flux Corrected Transport technique is utilized for the space charge density calculations.**

***Index Terms*—Corona discharge, dynamic simulation, Finite Element Method, Flux Corrected Transport**

I. Introduction

CORONA discharge studies have been undertaken for many years, not only because of the scientific interest in corona mechanism, but also because of its practical engineering importance [1]. Many industrial devices, such as electrostatic precipitators, ozone generators and others, use corona discharge [2], [3]. While in most cases a DC corona is generated, sometimes a pulsed corona discharge can lead to process improvement. The numerical simulation of the full dynamics of transient corona discharge is important for the optimization of these devices [4].

The majority of published studies dealt with the point-plane electrode systems and DC voltages rather than pulsed. This is because DC systems are much simpler for understanding and analysis. Corona systems with pulse energization are preferred in many applications because of lower power consumption and reduction of some parasitic effects, such as the back corona discharge. While some authors attempted simulation of the full corona dynamics, to date, no simple model of the electric corona discharge, valid for an arbitrary waveform of the applied voltage, has been presented.

Mengozzi and Feldman [5] developed a one dimensional time-dependent model of Trichel pulse development in a wire-cylindrical geometry. They simplified their model to avoid large-scale computations, and the model only considered 2-5μs energization pulses producing a single ionizing burst. Sekar [6] modeled the pulse corona discharge in a wire-cylinder geometry using the idea of charge shells. It was assumed that under Kaptzov's hypothesis, discrete charge shells were liberated during pulse discharge. Salasoo *et al*. [7] simulated corona in both space and time for a pipe type precipitator. Their model could estimate ion densities and field distribution for various pulse parameters.

Buccella [8] proposed a two-dimensional dynamic model to predict the *V-I* characteristics of a duct-type electrostatic precipitator operating under pulse energization. The electrostatic precipitator was divided in two distinct parts: one that is valid during the pulse-on period and uses the wave equation to calculate the electric field distribution and the second is valid during the pulse-off period and uses the continuity equation to calculate the space charge drift. The comparison of the results with experimental data showed a satisfactory agreement.

Meroth and others [9] presented a numerical model which was based upon a Finite Element approach for solving the Poisson equation and a non-stationary higher-order upstream Finite Volume scheme on unstructured grids for the transport equation. However, they assumed a model free of external convection and diffusion.

Liang et al. [10] presented a method for modeling a wire-cylinder ESP under pulse energization based on the characteristics of Trichel pulses and the applied pulse voltage. They included dust loading in their model and studied the interactions between ion space charge and particle charging, and their influence on the electric potential and field distributions. However, this model was 1-D and for single ionic species only.

Zhang and Adamiak [4] proposed a dynamic model for the negative corona discharge in the point-plane geometry. They used a hybrid Boundary-Element–Finite-Element Method technique to calculate the electric-field parameters, and the Method of Characteristics (MoC) for the charge-transport prediction. Their model could only predict an average corona current for variable voltage excitation and it was a pseudodynamic model.

In this paper, a numerical algorithm for the simulation of the dynamic corona discharge in air is proposed assuming single species charge carriers. The simulation results show the behavior of corona current and space charge density under two

Manuscript received April 17, 2009. This work was partially supported by the Natural Science and Engineering Research Council (NSERC) of Canada. The SHARCNET of Canada provided the computational resources.

P. Sattari is a Ph.D. student at the University of Western Ontario, London, Canada. (Phone: 519-661-2111, e-mail: psattari@uwo.ca).

G.S.P. Castle is retired but still associated with the Electrical and Computer Engineering Department, University of Western Ontario, London, Canada. (E-mail: pcastle@eng.uwo.ca).

K. Adamiak is with the Department of Electrical and Computer Engineering, University of Western Ontario, London, Canada. (E-mail: kadamiak@eng.uwo.ca).

waveforms of the applied voltage: step and pulse. The electric field is calculated by means of the Finite Element Method (FEM) and the hybrid FEM-Flux-Corrected Transport (FCT) technique is utilized for the space charge density calculations.

II. MATHEMATICAL MODEL

A. Governing Equations

Fig.1 shows a model for the negative corona discharge in the point-plane geometry. A hyperbolic needle is perpendicular to an infinitely large plate at a distance *d* with a tip radius curvature *R* and length *L*. Positive potential V_c is applied to the needle. An external resistance R_{ext} is connected in series with the needle and the ground plate. The ambient gas is air at room temperature and atmospheric pressure. Two different waveforms of the voltage: step and pulse-shaped can be applied. As this is a single species model, it is assumed that the ionization layer can be neglected and positive ions with average nobilities are assumed injected from the corona electrode.

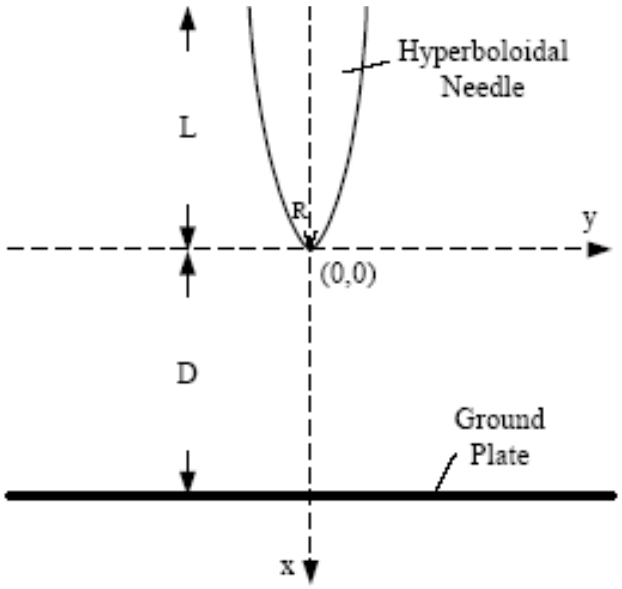

Fig.1. The configuration of corona discharge system.

In the absence of magnetic fields, the equations defining the electric field are:

$$\nabla \cdot \vec{D} = \rho \tag{1}$$

$$\nabla \cdot \vec{j} = -\frac{\partial \rho}{\partial t} \tag{2}$$

$$\vec{D} = \varepsilon_0 \vec{E} \tag{3}$$

$$\vec{E} = -\nabla V \tag{4}$$

$$\vec{j} = k\rho\vec{E} - D\nabla\rho \tag{5}$$

where $\vec{D}$ is the electrostatic displacement, ρ is the space charge density, $\vec{j}$ is the electric current density, ε_0 is the gas permittivity, $\vec{E}$ is the electric field, *V* is the electric potential and *k* is the mobility of charge carriers. At atmospheric pressure and room temperature, *k* is equal to 2×10^{-4} $m^2/V\cdot s$ [11].

D is the diffusion coefficient and is equal to [12]:

$$D = \frac{k_B T \cdot k}{e_0} \tag{6}$$

where k_B is the Boltzmann constant with is equal to 1.38065×10^{-23} $m^2kgs^{-2}K^{-1}$, *T* is the absolute temperature, e_0 is the electron charge, equal to 1.602×10^{-19} C.

Equations (3) and (4) can be used with (1) to obtain Poisson's equation

$$\nabla^2 V = -\rho/\varepsilon_0 \tag{7}$$

Equation (5) can be substituted into (2) to derive the continuity equation,

$$\frac{\partial \rho}{\partial t} + \nabla \cdot (k\rho\vec{E} - D\nabla\rho) = 0 \tag{8}$$

which can also be written in more detailed form as:

$$\frac{\partial \rho}{\partial t} + k\vec{E} \cdot \nabla\rho + \frac{k}{\varepsilon}\rho^2 - D\nabla^2\rho = 0 \tag{9}$$

B. Boundary conditions

The corona electrode and ground are equipotential. Therefore, the boundary conditions for voltage are:

$V = V_c$ on the corona electrode.
$V = 0$ on the ground plate.

The value of space charge density at different points of the corona electrode is the only required boundary condition for space charge density. Since the assumed model of the problem ignores the ionization process, it is impossible to derive the exact value of space charge density at different points of the corona electrode. The corona discharge starts as the field strength exceeds some threshold value, E_o. Therefore, the boundary condition for the charge density is usually replaced by the additional condition for the field strength on the corona electrode surface, $E(P) = E_o$, which can be related to the corona onset voltage, V_o [13].

In this case, it is assumed that the onset value of electric field on the corona electrode surface is obtained using Peek's formula, which in air is equal to [14]:

$$E_o = 3.1\times10^4 \delta \left(1 + \frac{0.308}{\sqrt{r_{eq}\delta}}\right)$$

where, $\delta = \frac{T_0 P}{T P_0}$, r_{eq} is the electrode equivalent radius of curvature in cm, T_0 is the standard temperature, *T* is the actual temperature, P_0 is the standard pressure and *P* is the actual pressure of gas. Peek's value varies along the electrode surface and depends on the equivalent radius of curvature of

electrode at each point.

III. NUMERICAL ALGORITHM

In this paper, an iterative algorithm is employed. For a given space charge density, the electric field is calculated by solving (7). The electric field varies strongly in both space and time. Near the discharge electrode the electric field variation is particularly steep, which demands a very fine spatial mesh, while in the remaining region the electric field variation is more uniform. A non-uniform spatial mesh is therefore essential for an accurate numerical treatment near the electrodes and the air gap.

In addition, the numerical algorithm for determining space charge density should fulfill the following requirements [15]:

1) It should give positive, accurate results, free from non-physical density fluctuation and numerical diffusion,
2) It should be computationally efficient,
3) It should be easily adopted for any geometry.

The first requirement is fulfilled by using a special method such as the Flux Corrected Transport which accurately represents the "real" diffusion in the system. The FCT method can capture the steep density gradients, without introducing spurious oscillations or artificial diffusion. In order to fulfill the last two requirements one has to use FEM as it offers computational efficiency through the use of unstructured grids. Therefore, a Finite Element version of FCT is used in this paper which can satisfy all the requirements [16].

At first, some initial space charge density on the corona electrode surface is assumed. When the applied voltage is larger than the corona onset value, (7) and (9) are solved iteratively for one time step and the charge density on the surface of the corona electrode is updated until the electric field on the electrode surface is equal to the Peek's experimental value. If the applied voltage decreases below the corona onset level, the surface charge density on the corona electrode is zero and the existing space charge moves towards the ground plate under the effect of the applied voltage which creates an electric field and pushes the space charge towards the ground.

The termination criteria of the iterative loops are the satisfaction of the following conditions:

1- The change of current in two successive iterations should be less than δ_1:

$$\frac{I_{k+1}-I_k}{I_{k+1}} \le \delta_1 \tag{10}$$

2- Summation of deviations of electric field on the corona tip nodes from Peek's value should be less than δ_2:

$$\sum_{i=tip\ nodes} \frac{\left(E_i - E_{peek,i}\right)^2}{E_{peek,i}^2} \le \delta_2 \tag{11}$$

IV. RESULTS

The hyperbolic needle is 1cm long (L=1cm) and is placed at 1cm above the ground plate (d = 1cm). The radius curvature R of the tip of the needle is 100μm. At the room temperature and atmospheric pressure the corona onset voltage for this configuration is evaluated to be 4.7 kV.

A. Step Voltage

A step voltage with the value of 10.0 kV is applied at t=0. The total corona current in the circuit with the external resistance of 50 MΩ is shown in Fig.2. This graph has been obtained assuming that δ_1 and δ_2 in (10) and (11) are 0.05 and 0.1, respectively. The upper electrode and the ground plate form a capacitor and, as a result, the system acts like a RC circuit.

The corona current can be calculated from [17]:

$$I = \frac{1}{V_0}\iiint \rho\vec{u}\cdot\vec{E}dv \tag{12}$$

where $\vec{u}$ is the velocity of the ions, $\vec{u} = k\vec{E}$, and V_0 is the voltage applied to the corona electrode.

At t=0, there is no space charge in the air gap. Therefore, a very large space charge should be injected from the corona tip in order to satisfy Kaptzov's hypothesis for the electric field and it results in a large current at t=0. As time increases, since space charge is accumulated in the air gap, less injected charge is required to keep the electric field equal to Peek's value and it results in electric current decreasing with time.

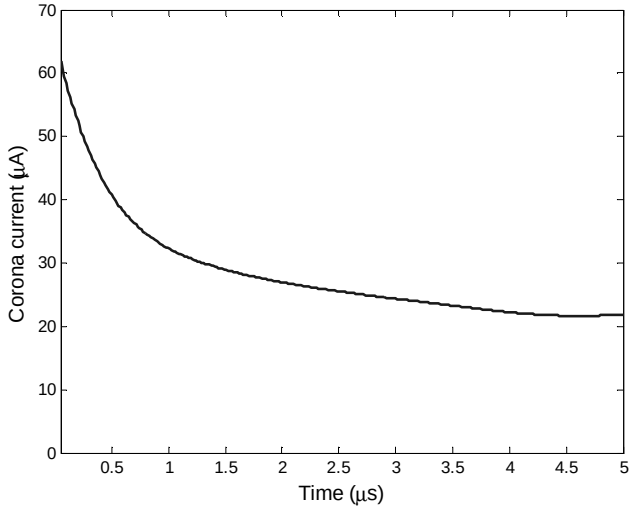

Fig.2. Corona current versus time (R_{ext} =50MΩ, V=10 kV)

Fig.3 shows the corona current versus time for two different external resistances. As expected, the value of current is larger for smaller external resistance. In Fig.4, corona current versus time for two different input voltages is shown. This figure shows that as expected a larger input voltage results in a larger current in the circuit.

Fig.5 shows the space charge density along the axis at six different instants of time. At t=160 ns, charge density is large and near the corona tip, but its value drops quickly along the

axis. As time goes on, charge travels towards the ground plate and, as the figure shows, it reaches the ground plate at about t=50 μs.

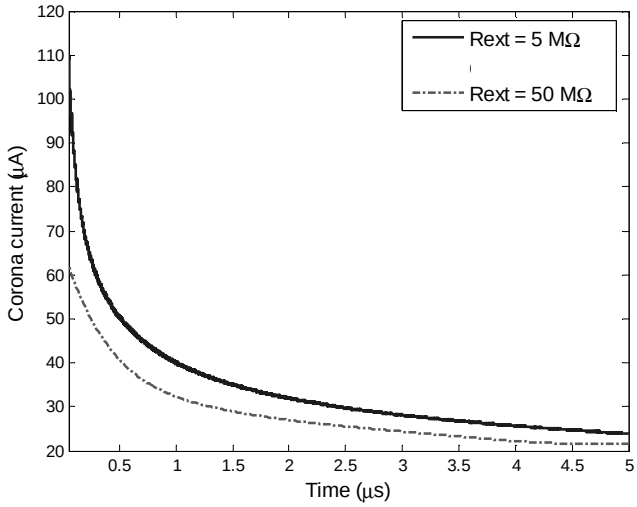

Fig.3. Corona current versus time for two different external resistances (V=10kV)

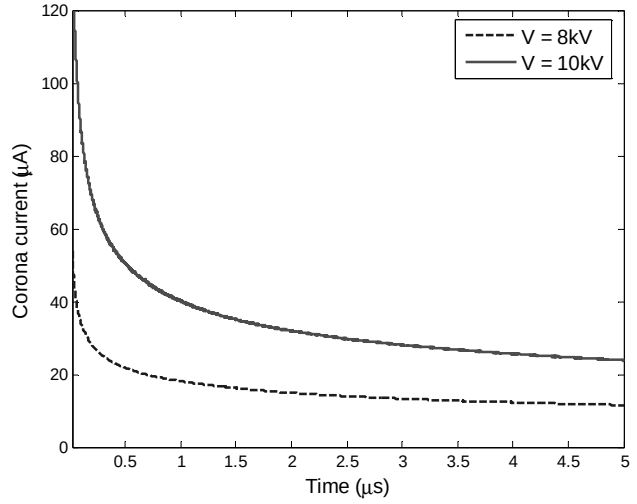

Fig.4. Current versus time for two different input voltages (R_{ext}=5MΩ)

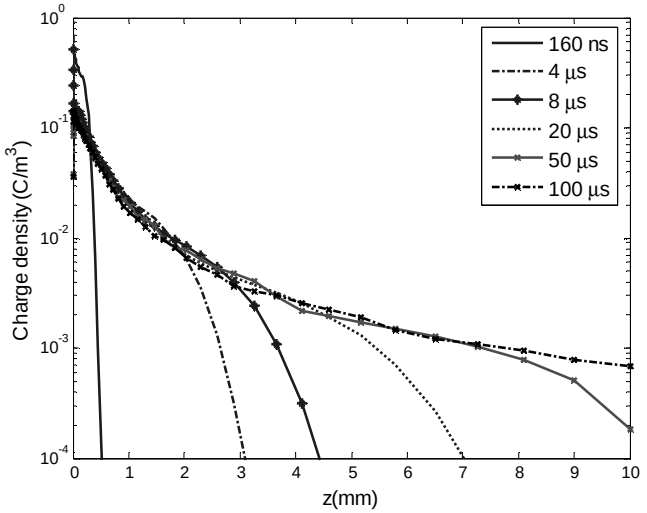

Fig.5. Space charge density along the axis of symmetry at six different instants of time (R_{ext}=50MΩ)

B. Pulse Voltage

In this section, a pulse shaped voltage with waveform shown in Fig.6 is applied to the corona electrode.

The pulse voltage waveform is generated using a double exponential function. The pulse parameters: the width of 300 ns, height of 6 kV (V_m=6 kV), and the rise time of t_m = 60 ns, are suitable for ESP applications [10]. The frequency of the pulses is chosen to be 5 kHz. This pulse voltage is superimposed on a dc voltage, which is set at a value below the corona onset voltage (i.e. 4kV).

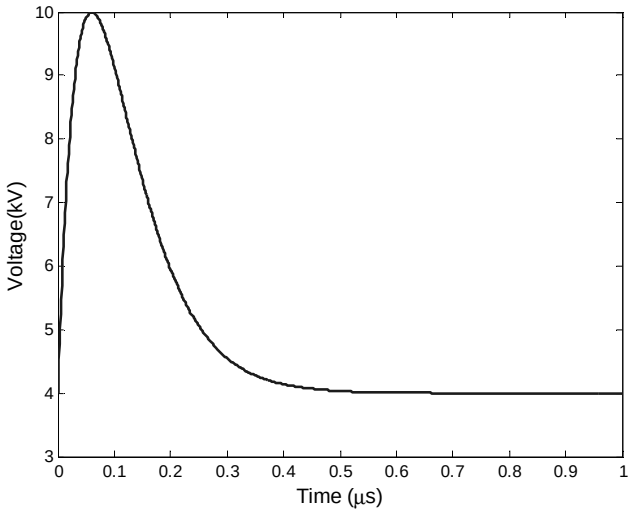

Fig.6. Applied pulse voltage described by

$$V_s(t) = \frac{V_m t}{t_m} e^{(1-t/t_m)} + V_{DC}$$

Fig.7 and 8 show the corona current and space charge density on the corona tip versus time. Total current is zero at t=0 and increases with applied voltage to a peak. Then, it starts decreasing and after some time only a small DC current (I=1.24 μA at t=1 μs) will remain in the circuit.

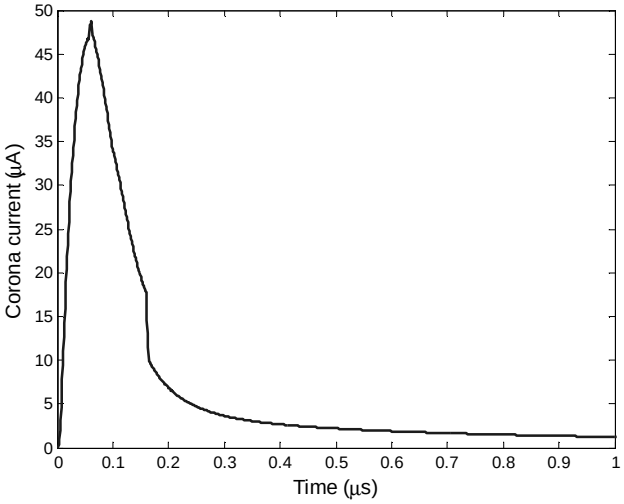

Fig.7. Corona current versus time (R_{ext} = 50MΩ)

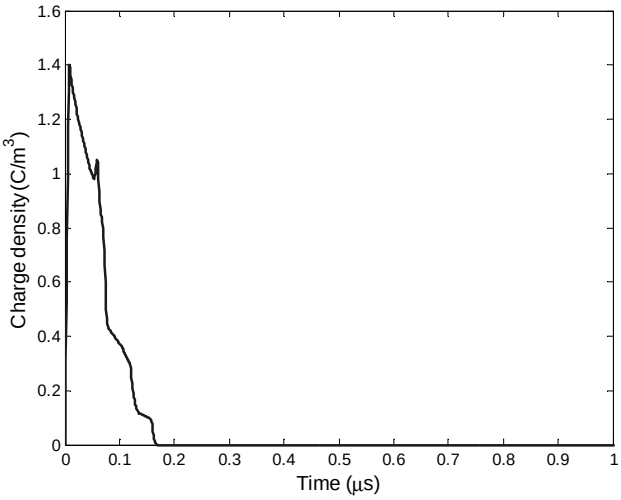

Fig.8. Space charge density on the tip of the corona wire versus time (R_{ext} = 50MΩ)

Fig.9 shows charge density along the axis of symmetry for five different time instants during and after the first voltage pulse. The ion cloud moves along the axis with time. At *t*=40 ns the ion cloud is near the tip and the value of space charge is large in this area. As time goes on, i.e. at *t*=10 μs, this cloud travels along the axis and charge becomes negligible near the tip. At *t*=100 μs and *t*=200 μs, the charge cloud gets further from the tip and its peak decreases.

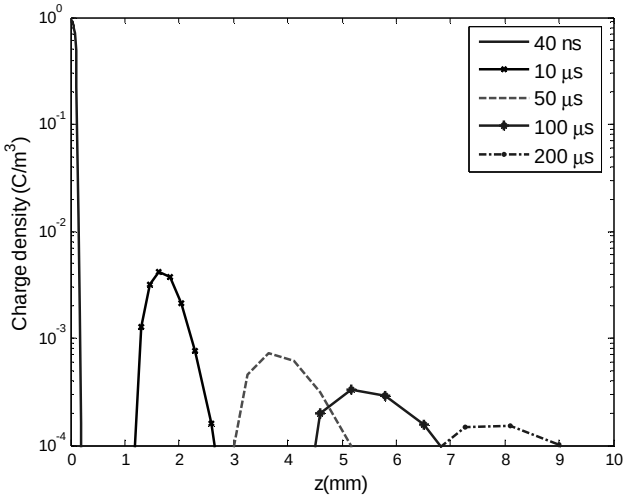

Fig.9. Charge density along the axis for five different time instants after the first voltage pulse (R_{ext} = 50MΩ)

Figures 10 and 11 show the distribution of the space charge density in the entire air gap at two time instants. At *t*=10μs, which is shortly after the first voltage pulse, the charge concentrates near the corona tip only.

At t = 210μs (Fig.11) there are two charge clouds. The smaller one is related to the first voltage pulse, which has traveled along the axis hence its value is decreased due to radial dispersion. The other one, with a larger peak value, is the one resulting from the second voltage pulse. Both of these clouds move along the axis with time with the velocity of $\vec{u} = k\vec{E}$. Since the value of electric field near the tip is large and decreases along the axis, the velocity of ion cloud decreases as it gets further from the tip. The cloud closer to the tip experiences a larger electric field, it initially moves faster than the other one and this decreases the distance between two pulses.

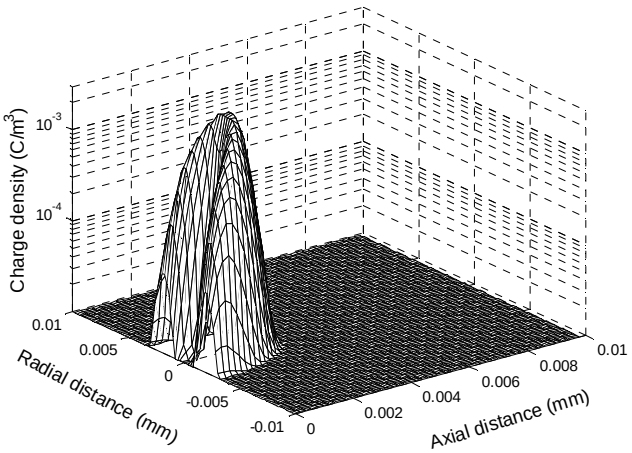

Fig.10. Charge distribution in the space at *t*=10μs (R_{ext} = 50MΩ)

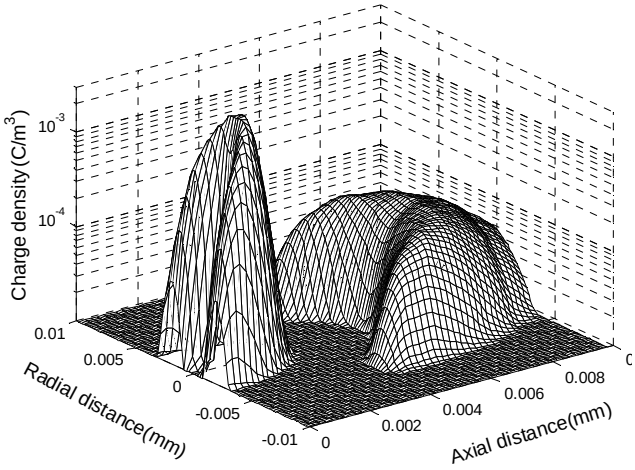

Fig.11. Charge distribution in the space at *t*=210μs (R_{ext} = 50MΩ)

Fig.12 shows the corona current versus time for two subsequent voltage pulses. When the applied voltage is below the corona onset level the corona discharge stops. In this period, the dc voltage (4kV in our case) produces an electric field, which moves the existing charges towards the ground producing a small DC current. The peak value of successive current pulses decreases only slightly from 48.75 μA to 48.4 μA. The decrement in the current peak in successive pulses results from the fact that as time goes on, the space charge density increases in the air gap. This increment of the space charge, decreases the electric field and decreases the peak of successive pulses of corona current.

To better show the effect of space charge on the peak value of current with time, the frequency of the pulse has been increased from 5 kHz to 50 kHz. Fig.13 shows the corona current versus time for five applied voltage pulses. The current peak values are 48.75, 46.97, 45.82, 44.98, 42.5 μA, respectively.

The average current in each case is also calculated using the formula:

$$I_{av} = \frac{1}{T_P}\int_0^{T_P} Idt$$

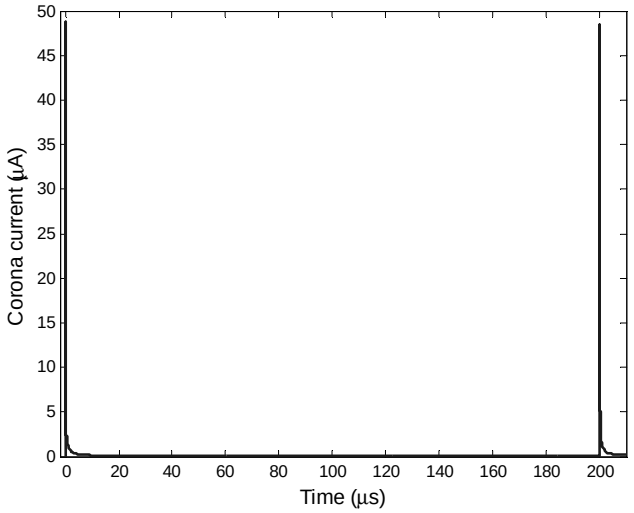

Fig.12. Corona current versus time (R_{ext} = 50MΩ)

This value is calculated to be 0.0728 μA and 0.5624 μA for f=5 kHz and f=50 kHz, respectively. As expected, the average current increases as the frequency is increased although not in direct proportion.

Fig.14 shows the distribution of the space charge density at t=41 μs in the entire air gap for frequency f=50 kHz. At this time, three pulses have been applied to the corona electrode. This figure shows that if the frequency of the applied voltage is too high, the charge pulses will practically combine.

V. CONCLUSIONS

In this paper, a hybrid FEM-FCT dynamic model for simulating electric corona discharge has been proposed. The results show the behavior of the corona current and space charge density for two different waveforms of the voltage: step and pulse.

In DC corona, the total corona current and space charge density have large values at t=0, but they decrease quickly to a constant value at steady state. It was also shown that as expected, larger input voltage results in a larger current in the circuit and the value of current is larger for smaller external resistance.

When a periodic pulse voltage is applied to the corona electrode, the resulting current will be periodic, too. The average current depends on the frequency and increases as the frequency of pulses increase. It was shown that the peak value of these sequential current pulses decreases. This results from the fact that as time goes on, space charge is accumulated in the air gap, and increased space charge decreases the value of electric field. A decrease in electric field value results in decreasing the peak of successive pulses of the corona current. When a pulse voltage is applied, the current increases quickly to a peak value and then decreases to a small DC value, when the applied voltage is below the corona onset voltage. The charge clouds are formed in the air gap and move towards the ground plate. The velocity of these charge pulses depends on the electric field. So, as they move, their velocity decreases due to the decrease in the electric field along the axis. It follows that if the frequency of the applied pulse voltage is too high, charge pulses will eventually combine.

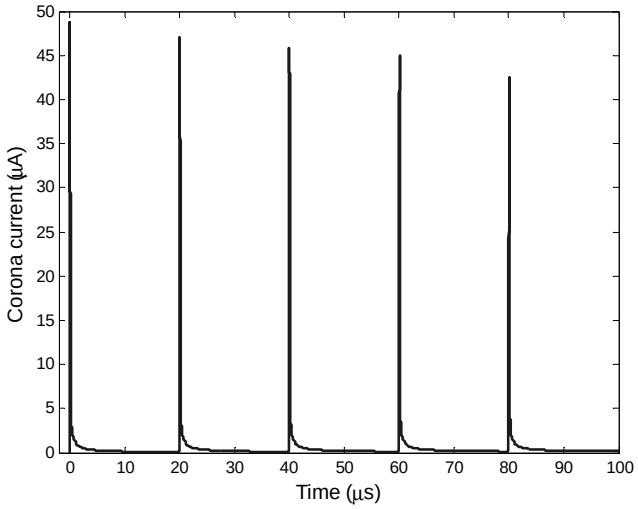

Fig.13. Corona current versus time (R_{ext} = 50MΩ)

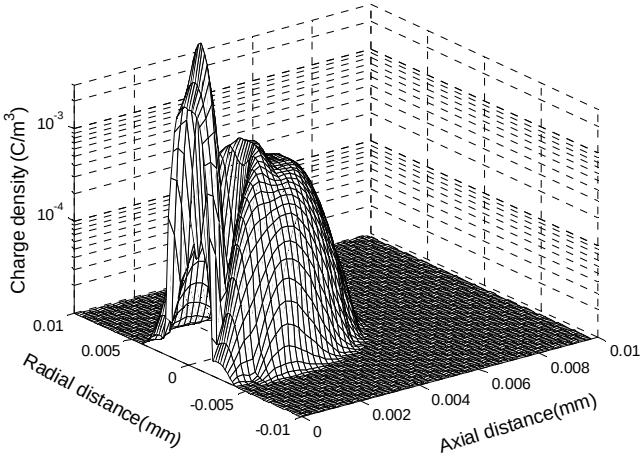

Fig.14. Charge distribution in the space at t=41 μs

REFERENCES

[1] C.H. Zhang and J.M.K. MacAlpine, "A phase related investigation of ac corona in air," *IEEE Trans. on Dielectr. and Electr. Insul.*, vol. 10, no. 2, pp. 312-319, April 2003.

[2] J. S. Chang, A. J. Kelly, and J. M. Crowley, *Handbook of Electrostatic Processes*, NY: Marcel-Dekker, 1995.

[3] J.S. Chang, P.A. Lawless, and T. Yamamoto, "Corona discharge processes," *IEEE Trans. on Plasma Sci.*, vol. 19, no. 6, pp. 1152-1166, Dec. 1991.

[4] J. Zhang and K. Adamiak, "A dynamic model for negative corona discharge in point-plane configuration," *Proc. of ESA/IEJ/IEEE-IAS/SFE Joint Conference on Electrostatics*, Berkeley, California, vol. 2, pp. 588-597, June 2006.

[5] L. N. Menegozzi and P. L. Feldman, "The physics of pulse energization of electrostatic precipitators," *Proc. at the 3rd Symp. Transfer and Utilization of Particulate Control Technology*, Orlando, FL, Mar. 1981.

[6] S. Sekar, "An investigation of pulsed corona in cylindrical and wire-plate geometries," *J. Electrostat.*, vol. 13, pp. 29-41, 1982.

[7] L. Salasoo and J. K. Nelson, "Simulation and measurement of corona for electrostatic pulse powered precipitators," *J. Appl. Phys.*, vol. 58, no. 8, pp. 2949–2957, Oct. 1985.

[8] C. Buccella, "Computation of V-I characteristics of electrostatic precipitators," *J. Electrostat.*, vol. 37, pp. 277–291, 1996.
[9] A. M. Meroth, T. Garber, C.D. Munz, P.L. Levin, A.J. Schwab, "Numerical solution of nonstationary charge coupled problems," *J. Electrostat.*, vol. 45, pp. 177-198, 1999.
[10] X. Liang, S. Jayaram, A. Berezin, et al. "Modeling of the electrical parameters of a wire-cylinder electrostatic precipitator under pulse energization," *IEEE Trans. on Ind. Appl.*, vol. 38, no. 1, pp. 35–42, 2002.
[11] B. Eliasson and U. Kogelschatz, *Basic Data for Modeling of Electrical Discharges in Gases: Oxygen*, Bown Boveri Technical Report, 1986 (unpublished).
[12] P. A. Va'zqueza, A. T. Pe'rez, A. Castellanos and P. Atten, "Dynamic of electrohydrodynamic laminar plumes: scaling analysis and integral model," *Phys. Fluids*, vol. 12, no. 11, pp. 2809-2818, 2000.
[13] K. Adamiak, V. Atrazhev, P. Atten, "Corona Discharge in the Hyperbolic Point-plane Configuration: Direct Ionization Criterion versus Approximate Formulations," *IEEE Trans. on Dielectr. and Electr. Insul.*, vol. 12, no. 5, pp. 1025-1034, October 2005.
[14] K. Adamiak and P. Atten, "Simulation of corona discharge in point-plane configuration," *J. of Electrostat.*, vol. 61, pp. 85-94, 2004.
[15] G. E. Georghiou, R. Morrow, and A. C. Metaxas, "An Improved Finite-Element Flux-Corrected Transport Algorithm," *J. of Comput. Phys.* vol.148, pp. 605-620, 1999.
[16] R. Loehner, *Applied Computational Fluid Dynamics Techniques: An Introduction Based on the Finite Element Method*, John Wiley and Sons, 2001.
[17] N. Sato, "Discharge current induced by the motion of charged particles," *J. Phys. D: Appl. Phys.* vol.13, no. 1, pp. L3-L6, 1980.